International Journal of Engineering & Technology, 7 (3.20) (2018) 677-682

International Journal of Engineering & Technology

Website: www.sciencepubco.com/index.php/IJET

Research pape

Stability Analysis of A Third Order DC to DC Converter by Considering Input Current as Output Vector

J. Barnabas Paul Glady[1]*, K. Manjunath[2]

[1] *Research Scholar*
Sathyabama Institute of Science and Technology, Chennai India
[2] *HOD EEE Department, SDMIT Ujirie, India*
**Corresponding author E-mail:kmanjunathsdmit@gmail.com*

Abstract

Luo converters are used in various application because of low ripple, high voltage gain with less number of components. In the literature Luo converter was analysed for voltage gain, output voltage control etc. but the stability of the third order system was not analysed. In this paper the stability was analysed by root locus method. Initially the state space modelling was applied by considering input current as the output vector and the input to output transfer function is obtained. The transfer function reveals that the third order system falls under the category of marginally stable system. In order to bring it in to a stable system a PID controller was designed for the third order system. The performance of the PID system for the third order system was compared with that of the transfer function when it was split in to first order and second order transfer function. For the marginally stable second order transfer function a PID controller, lead compensator and notch filter was designed. The split transfer function performance of lead, notch filter was compared with the PID of the third order system.

Key words: *Luo converter, state space averaging, root locus, transfer function, PID controller, Lead compensator, notch filter*

1. Introduction

Dc to dc converters are widely used in application like battery charging , switched mode power supply, renewable energy , electric vehicle ,electric drive etc. in all this application they are used for boosting and bucking operation. The boost action will improve the voltage level and the buck action will decrease the voltage level. For boost action to be performed in dc to dc converters there are various categories like non isolated, isolated, unidirectional, bi directional, voltage fed, current fed, hard switched, soft switched and minimum phase category. Similarly there are various techniques for boost action like charge pump, voltage multiplier, magnetic coupling, multistage level and voltage lift techniques. The voltage lift techniques is used in many converters like luo, cuk, sepic and zeta converters. In voltage lift technique a capacitor is charged to a specific voltage like input voltage and then step up the output voltage with the help of voltage level of pre charged capacitor. This process can be repeated by including additional capacitor resulting in invention of re-lift, triple-lift and quadruple lift circuits.

In the literature the luo converter was introduced [1] in 2003. After that a cascaded Luo converter was introduced in order increase the voltage gain in geometric progression doubled with reduced components. Then soft switching was introduced in [3] ,[4] & [13] in order to increase the efficiency of the converter. The zero voltage switching was done by using quasi resonant converter. [5] Discuses about output voltage regulation of the converter by PI control and PWM based sliding mode control. Sliding mode control was implemented to Luo converter for current distribution [6] by paralleling of the converter. [7] discusses about the hysteresis based sliding mode control of Luo converter.[8],[9] & [12] discusses about the current mode control and dual loop control for regulating the output voltage [13],[14] and output current of the Luo converter . Hence the stability of the luo converter was not analysed [15].

2. State Space Averaging of Positive Output Elementary Super Lift Luo Converter

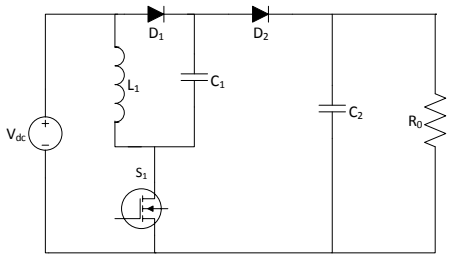

Figure 1: Circuit Diagram of Luo Converter

Figure 1 shows the circuit diagram of positive output elementary Luo converter. It contains one voltage source V_{dc}, one inductor L_1, two capacitor C_1 and C_2, two diodes D_1 and D_2, one switch S_1 and one load Resistor R_o. The Luo converter is boost type of geometric progression.

Let the state variables be defined as

$$X(t) = \begin{bmatrix} I_{L1}(t) \\ V_{C1}(t) \\ V_{C2}(t) \end{bmatrix} \quad (1)$$

Copyright © 2018 Authors. This is an open access article distributed under the Creative Commons Attribution License, which permits unrestricted use, distribution, and reproduction in any medium, provided the original work is properly cited.

The input vector be input voltage

$$U(t) = V_{dc}(t) \tag{2}$$

The output vector be load current

$$Y(t) = I_{dc}(t) \tag{3}$$

The state equation of the system is given

$$\dot{X}(t) = AX(t) + BU(t) \tag{4}$$

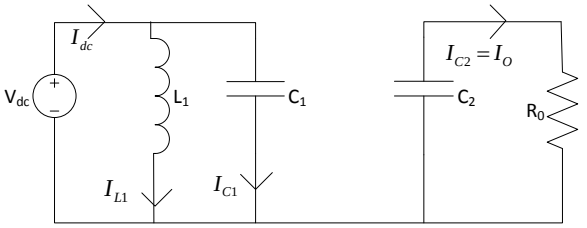

Figure 2: Equivalent Circuit Diagram of Mode I

The mode I equivalent circuit is shown in figure 2. In mode I the switch mosfet is turned on. When mosfet is turned on the inductor L_1 and C_1 will come in parallel with voltage source V_{dc}. A current I_{dc} will flow from the battery to the inductor and capacitor. The current flowing in the inductor is shown as I_{L1} and the current flowing in the capacitor is shown as I_{c1}.During this time the inductor will store the energy as magnetic field and the capacitor will store the energy as electric charge. At the same time the output capacitor will discharge I_o the stored energy to the load resistor R_o as shown in the diagram.
Writing the KVL equation for the state variables

$$Y(t) = CX(t) + EU(t) \tag{5}$$

$$V_{L1}(t) = L\frac{di_{L1}}{dt} = V_{C1}(t) \tag{6}$$

Current through the Capacitor C_1 Is Given By

$$I_{c1}(t) = C_1\frac{dV_{C1}(t)}{dt} = I_{dc}(t) - I_{L1}(t) = \frac{V_{dc}(t)}{R_{dc}} - I_{L1}(t) \tag{7}$$

Current through the capacitor C_2

$$I_{C2}(t) = C_2\frac{dV_{C2}(t)}{dt} = -\frac{V_{C2}(t)}{R_O} \tag{8}$$

Writing the state equation for mode I

$$\begin{bmatrix} L_1 & 0 & 0 \\ 0 & C_1 & 0 \\ 0 & 0 & C_2 \end{bmatrix}\frac{d}{dt}\begin{bmatrix} I_{L1}(t) \\ V_{C1}(t) \\ V_{C2}(t) \end{bmatrix} = \begin{bmatrix} 0 & 1 & 0 \\ -1 & 0 & 0 \\ 0 & 0 & -\frac{1}{R_O} \end{bmatrix}\begin{bmatrix} I_{L1}(t) \\ V_{C1}(t) \\ V_{C2}(t) \end{bmatrix} + \begin{bmatrix} 0 \\ \frac{1}{R_{dc}} \\ 0 \end{bmatrix}V_{dc}(t) \tag{9}$$

The output state equation is given by

$$I_{dc}(t) = \begin{bmatrix} 1 & \frac{1}{R_{C1}} & 0 \end{bmatrix}\begin{bmatrix} I_{L1}(t) \\ V_{C1}(t) \\ V_{C2}(t) \end{bmatrix} + [0]V_{dc}(t) \tag{10}$$

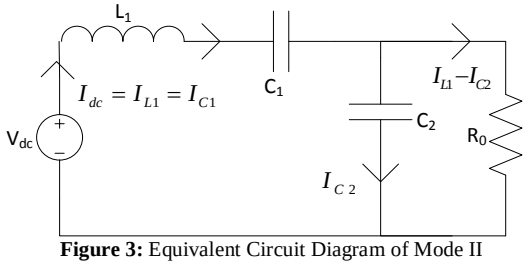

Figure 3: Equivalent Circuit Diagram of Mode II

The mode ii equivalent circuit diagram is shown in figure 3. In this mode the mosfet is turned off. When mosfet is turned off the voltage source V_{dc}, the inductor L_1, capacitor C_1 and C_2 will be forming a loop as shown in the diagram above. In this case the inductor L_1 and C_1 will be releasing the stored energy and the capacitor C_2 will be storing the energy. During this period the load will be supplied by the source V_{dc} as shown in the diagram.
The voltage across the inductor is given by

$$V_{L1}(t) = L_1\frac{dI_{L1}(t)}{dt} = V_{C2}(t) - 2V_{dc}(t) \tag{11}$$

The current through the capacitor c is given by

$$C_1\frac{dV_{C1}(t)}{dt} = I_{L1}(t) \tag{12}$$

The current through the capacitor c is given by

$$C_2\frac{dV_{C2}(t)}{dt} = I_{L1}(t) - \frac{V_{C2}(t)}{R_O} \tag{13}$$

Writing the state equation for mode II

$$\begin{bmatrix} L_1 & 0 & 0 \\ 0 & C_1 & 0 \\ 0 & 0 & C_2 \end{bmatrix}\frac{d}{dt}\begin{bmatrix} I_{L1}(t) \\ V_{C1}(t) \\ V_{C2}(t) \end{bmatrix} = \begin{bmatrix} 0 & 1 & 0 \\ 1 & 0 & 0 \\ 1 & 0 & -\frac{1}{R_O} \end{bmatrix}\begin{bmatrix} I_{L1}(t) \\ V_{C1}(t) \\ V_{C2}(t) \end{bmatrix} + \begin{bmatrix} -2 \\ 0 \\ 0 \end{bmatrix}V_{dc}(t) \tag{14}$$

The output state equation for mode II

$$I_{dc}(t) = I_{L1}(t) \tag{15}$$

$$I_{dc}(t) = \begin{bmatrix} 1 & 0 & 0 \end{bmatrix}\begin{bmatrix} I_{L1}(t) \\ V_{C1}(t) \\ V_{C2}(t) \end{bmatrix} + [0]V_{dc}(t) \tag{16}$$

The input to output transfer function is given by

$$Y = C(SI - A)^{-1}B \tag{17}$$

$$Y = \frac{S^2\left[\frac{D}{C_1R_{C1}R_{dc}} - \frac{2D^*}{L_1}\right] + S - \left[\frac{2D^*}{L_1C_2R_O} + \frac{D(D-D^*)2D^*}{L_1C_1R_{C1}} + \frac{D}{C_1L_1R_{dc}} + \frac{D^2}{C_1C_2R_OR_{dc}R_{C1}}\right] + \frac{2D^*D(D-D^*)}{L_1C_1C_2R_{C1}R_O} + \frac{D}{L_1C_1C_2R_OR_{dc}}}{S^3 + \frac{S^2}{C_2R_0} + S\frac{(D-D^*)}{L_1C_1} + \frac{(D-D^*)}{L_1C_1C_2R_O}} \tag{18}$$

3. Study of Output to Input Transfer Function

For equation (18) the values given in table 1 are substituted to obtain the input to output transfer function of the system. The input to output transfer function obtained is given by

$$\frac{2.73424e05s^2 + 1.919e8s + 5.425e8}{s^3 + 1000s^2 + 40000s + 4e7} \quad (19)$$

Table 1 shows the values used for the transfer function

Parameters	Values
Duty cycle D	0.7
Inductor L1	100mh
Capacitor C1 and C2	100uf
Internal resistance of capacitor Rc1 and Rc2	0.16
Output resistance	10

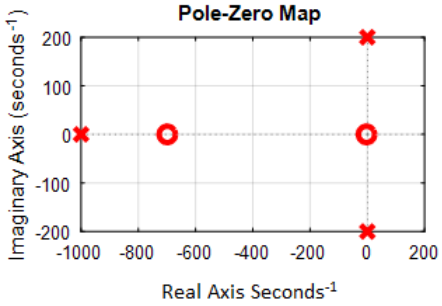

Figure 4: Pole Zero Map of Transfer Function

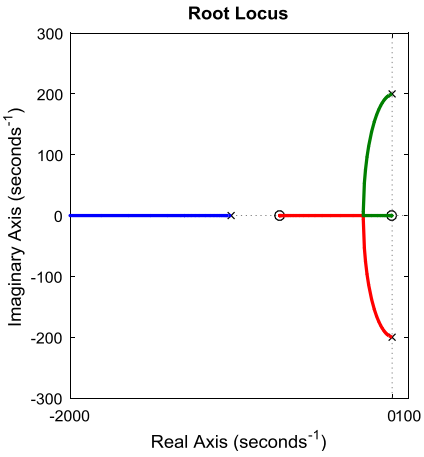

Figure 5: Root Locus of the Output to Input Transfer Function

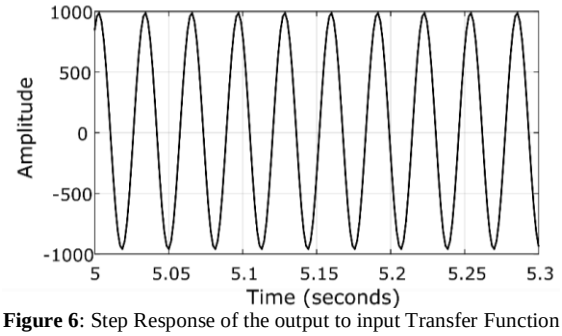

Figure 6: Step Response of the output to input Transfer Function

The pole zero map of the input to output system is shown in figure 4. It shows that the system is marginally stable system. In the pole zero map we find that there are 3 poles and two zeros. One pole is real and two poles are imaginary. The real pole lies at -1000 and the imaginary poles lies at 200i and -200i.The step response of the system is sinusoidal in nature proving it marginally stable system as shown in figure 6. The root locus of the system is shown in the figure 7.

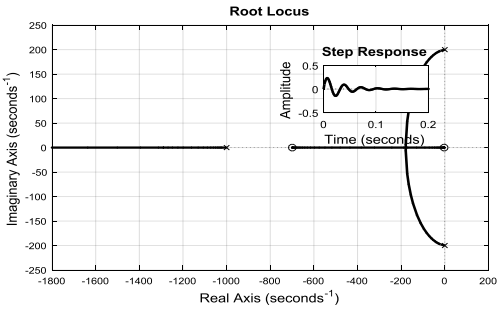

Figure 7: Root Locus and Step Response of Transfer Function for Gain Of 0.00029937

Now the stability of the system is analyzed by root locus method. In root locus method the gain of the system is increased in order to bring the system in to stability. Initially the gain is increased to 0.00029937 to check the change of response. The step response and the root locus of the third order system are shown in figure 7. It gives a settling time of 0.139, peak response of 0.236, rise time of 0.516micro second and steady state final value of 0.00404. Since the gain value is very low the steady state value also low.

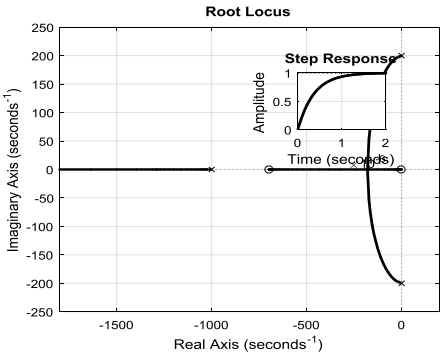

Figure 8: Root Locus and Step Response of Transfer Function for Gain of 10

Now when gain value is increased to 10 the settling time is 1.32 micro second, rise time is .78 micro second, peak over shoot is 0.621% and final steady state value is 0.996 which is shown in figure 8. Now when gain value is increased to 100 the settling time is 0.142 micro second, rise time is 0.008 micro second, peak over shoot is 0% and final steady state value is 0.996 which is figure 9.

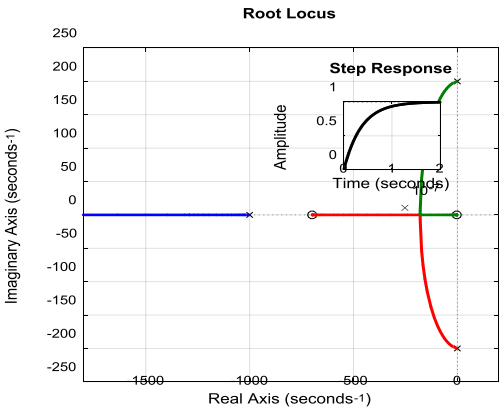

Figure 9: Root Locus and Step Response of Transfer Function For Gain of 100

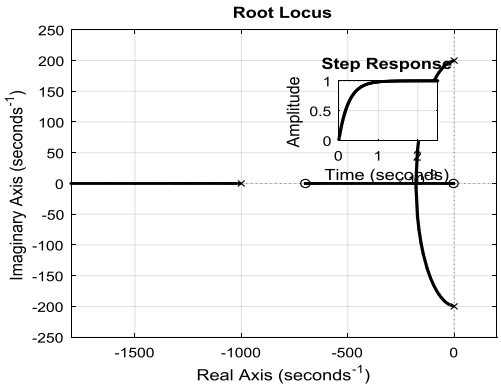

Figure 10: Root Locus and Step Response of Transfer Function for Gain 1456

Now when the compensator value is increased to 1456 the rise time is .543nano seconds, the settling time is 0.968 Nano seconds and final value is1 which is shown in figure 10. Even though the settling time was decreased to nanoseconds practically it is difficult to implement for creating such a high gain circuit.

4. Analysing the Splitted Transfer Function

The second part of analysis involves splitting the transfer function in to first order and second order transfer function and analyzing them separately. When the transfer function is split in to two the first order is given by $\frac{78922}{S+1000}$. And the second order transfer function is given by $\frac{9.500419e9}{S^2+40000}$. The first order equation gives pole located at left side of the plane. While the second order transfer function gives poles located at the imaginary axis of the s-plane. The first order pole gives stability to the system while the second order pole causes the instability to the system. The step response of the first order system is shown in figure 11. The step response is a stable response giving a settling time of 3.912milli seconds, rise time of 2.2milli seconds and the steady state value is 78.9.

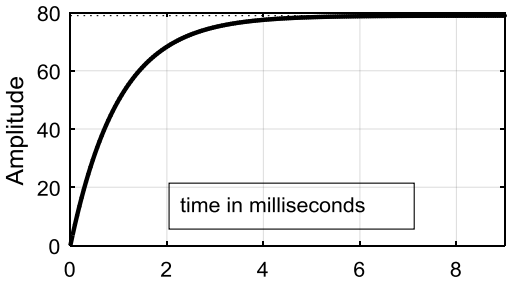

Figure 11: Step Response of First Order System

Table 2 PID values

Parameters	Values
P	5.827e-5
I	0.0051526
D	1.4365e-7
N	15224.1787
Rise time	0.000921 seconds
Settling time	0.0191 seconds
overshoot	14.6%
Peak value	1.15

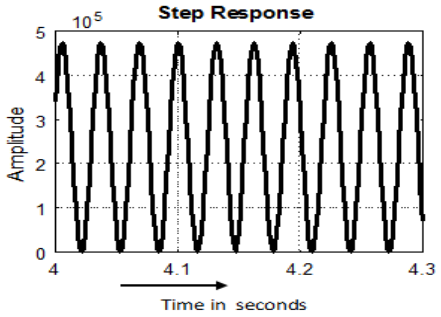

Figure 12: Step Response of Second Order System

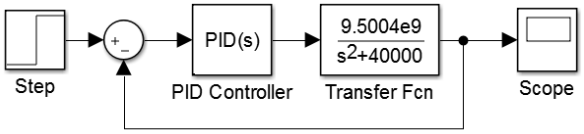

Figure 13: Second Order System with PID controller

And the second order transfer function is $\frac{9.500419e9}{S^2+40000}$. The response of the second order system is oscillatory in nature and the oscillation is constant and hence the system is marginally stable which is shown in figure 12. In order to bring stability to second order system a PID control was designed. The response of the system is stable after introducing the controller. The second order system and the PID control is shown in figure 13. The PID values and the characteristics of the second order response values are given in table no.1. The PID values are selected for creating a settling time of 20 milli seconds and the simulation achieves a settling time of 19.1 milli seconds creating a peak value of 1.15 and an over shoot of 14.6%. The step response of the second order system is shown in figure 14.

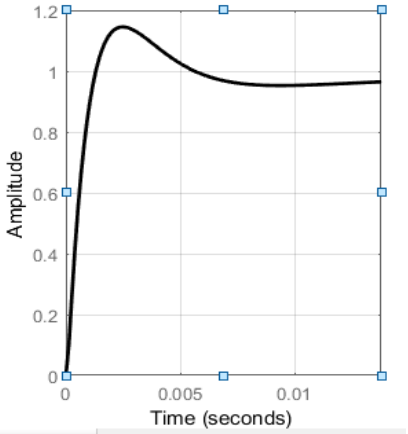

Figure 14: Tuned Response of Second Order System

In the third way of analysis a zero is added to the root locus of the second order system. The root locus of the second order system is shown in figure 15. There are two poles present in the imaginary axis and travel to infinity along the imaginary axis. If zero is added the poles direction will change and the system may become a stable system.

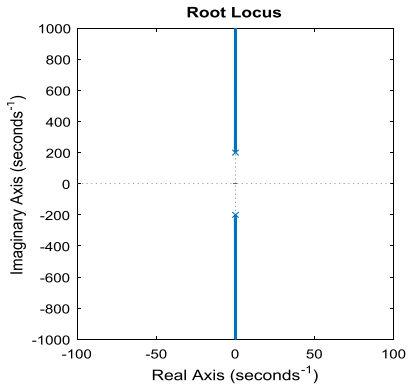

Figure 15: Root Locus of Second Order System

When zero is added at -10, and -100 the root locus of the second order system changes as shown in figure 13 and figure 14 respectively.

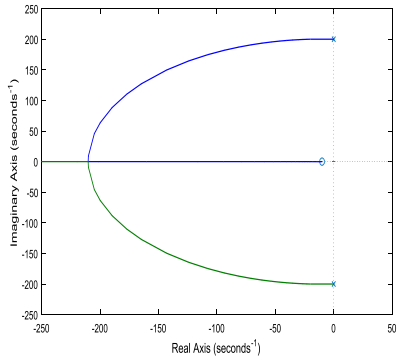

Figure 16: Root Locus of Second Order System When Zero Is Added At -10

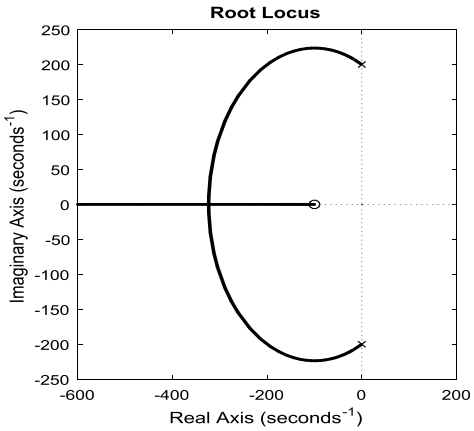

Figure 17: Root Locus of Second Order System When Zero Is Added At -100

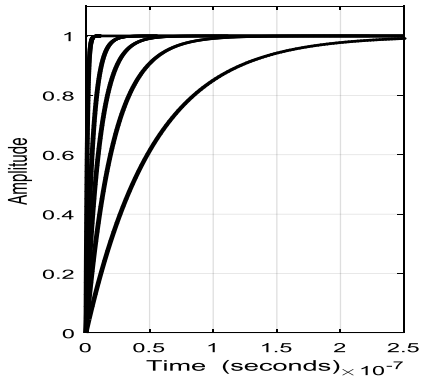

Figure 18: Step Response of Second Order System When Position of Zero Is Changed -10 To -500

When zero is added in the root locus at -10,-50,-100,-200and -500 of the LHP of the plane the step response is shown in figure 15 , it is observed that the settling time of the step response decreases as shown in the table as the farther the distance of zero with respect to the origin.

Now when the zero is located at -10 and the gain of the compensator alone increased from 1, 10, 50, 100, the step response of the system is shown in figure 21.

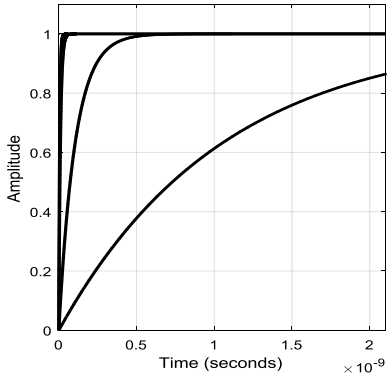

Figure 19: Step Response of Second Order System When Zero Is Located At -10 and Gain Is Increased From 1 to 100

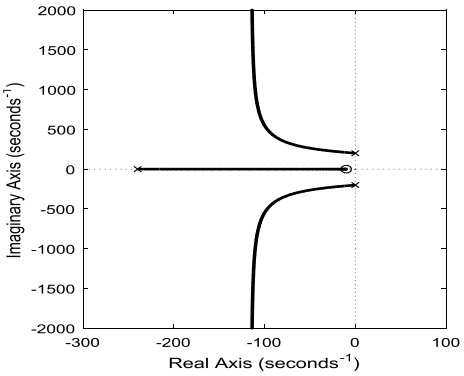

Figure 20: Root Locus of Second Order System When Lead Compensator Is Designed

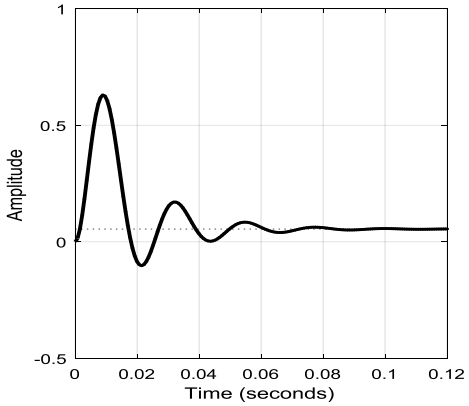

Figure 21: Step Response of the System for Second Order with Lead Compensator

When a lead compensator $\frac{(1+0.1s)}{(1+0.0042s)}$ which has a zero at -10 and pole at -240 the root locus is shown in figure 17. The step response of the second order system with lead compensator is shown in figure 18. The settling time given by the lead compensator is 0.0686 second, peak overshoot of 1.05e3 and a rise time 0.00112 second.

Similarly a notch filter was designed to check the performance of the system. The notch filter is given by $\frac{(1+0.0011s+0.0014s^2)}{(1+0.0019s+0.0014s^2)}$.

The location of pole is at -266±647j. The zero location given by-100,100. To improve the performance of the notch filter a zero was added at 1. The designed notch filter with gain of 10 gives a settling time of 4.12 Nano seconds, rise time of 2.31 Nano seconds with no over shoot. When the second order system is added with first order system the table 2 gives the performance of the system. The step response of the notch filter without gain and with gain of 10 is shown in figure 20 and 21. The gain in the notch filter eliminates the overshoot completely and gives a smooth curve as shown in figure 21. The table 2 shows the performance of various controllers with respect to the various parameters. It is found that the notch filter gives the best performance with respect to other filters.

Table 3: Performance of various compensators

Parameters	First Order	Second Order		
		PID	LEAD	NOTCH
Settling Time	3.92ms	19.1ms	68ms	4.12e-6 ms
Rise Time	2.2ms	0.921ms	1.12ms	2.31e-6 ms
Peak Over Shoot	-	14.6%	1.05e3%	-

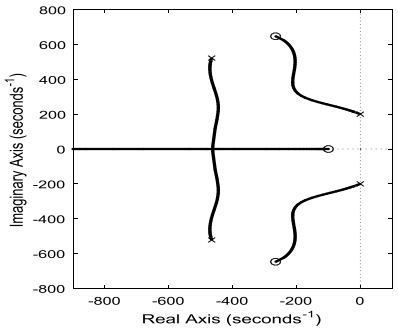

Figure 22: Root Locus of the Second Order System with Notch Filter

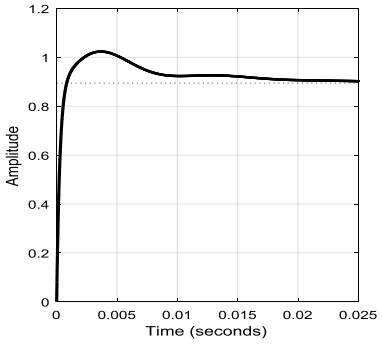

Figure 20: Step Response of the System for Second Order System with Notch Filter

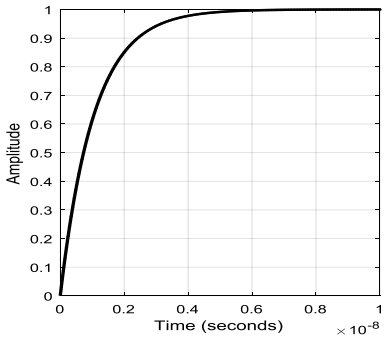

Figure 23: Step Response of Second Order System with Notch Filter and Gain As 10

5. Conclusion

In this paper the stability of the Luo converter was analysed by root locus method. The converter system is modelled by state space averaging method and the input to output transfer function is obtained. The transfer function is analysed for the stability of the system. It is found that the system is marginally stable system because two poles lie on the imaginary axis. For this system to become stable a PID controller, lead compensator, a notch filter was designed. It is found that notch filter gives the best performance compared to other controllers.

References

[1] F.L.Luo and H.Ye, "Positive output super lift converters," IEEE Transaction on power electronics, Vol.18, No. 1, pp. 105-113, January 2003.

[2] Positive output cascade boost converters F. L. Luo; H. Ye IEE Proceedings - Electric Power Applications Y ear: 2004, Volume: 151, Issue: 5 Pages: 590 - 606

[3] Analysis, design and control of zero-voltage switching quasi-resonant-positive output super lift Luo converter E. Jayashree; G. Uma IET Power Electronics Year: 2011, Volume: 4, Issue: 1 Pages: 21 – 28

[4] Design and implementation of zero-voltageswitching quasi-resonant positive-output Luo converter using analog resonant controller UC3861 E. Jayashree; G. Uma IET Power Electronics Year: 2011, Volume: 4, Issue: 1 Pages: 81 - 88

[5] PI and PWM Sliding Mode Control of POESLL Converter Hadi Nasiri Jazi; Alireza Goudarzian; Rohallah Pourbagher; Sayed Yaser Derakhshandeh IEEE Transactions on Aerospace and Electronic Systems Year: 2017, Volume: 53, Issue: 5 Pages: 2167 – 2177

[6] K. Ramash Kumar and S. Jeevananthan, "A Sliding Mode Control for Positive Output Elementary Luo Converter," Journal of Electrical Engineering, Vol.10, No.4, pp. 115-127, December 2010.

[7] K. Ramash Kumar and S. Jeevananthan," Hysteresis Modulation Based Sliding Mode Control for Positive Output Elementary Super Lift Luo Converter", International Journal of Electrical and Electronics Engineering 2:3. pp 131-138, 2009.

[8] K.Ramash Kumar and S.Jeevananthan, "Sliding Mode Control for Current Distribution Control in Paralleled Positive Output Elementary Super Lift Luo Converters", Journal of Power Electronics, vol. 11, no.5-3, pp.639-654, 2011.

[9] Comparative study of current-mode controllers for the positive output elementary Luo converter via state-space and frequency response approaches Satyajit Hemant Chincholkar; Chok-You Chan IET Power Electronics Year: 2015, Volume: 8, Issue: 7 Pages: 1137 - 1145

[10] Implementation of dual-loop controller for positive output elementary luo converter Shama Ravichandran; Sanjib Kumar Patnaik IET Power Electronics Year: 2013, Volume: 6, Issue: 5 Pages: 885 – 893

[11] Hybrid split capacitors and split inductors applied in positive output super-lift Luo-converters Fang Lin Luo; Hong Ye IET Power Electronics Year: 2013, Volume: 6, Issue: 9 Pages: 1759 – 1768.

[12] Ayyappa Swamy, Y,G. Nagarajan, "Implementation of Non-Isolated High Voltage Gain Input-Parallel Output-Series Dc/Dc Converter with Switched Capacitor" Volume 8 (5),pp 2111-2118,2015.

[13] MuhammedShafi. P,Selvakumar.S*, Mohamed Shakeel.P, "An Efficient Optimal Fuzzy C Means (OFCM) Algorithm with Particle Swarm Optimization (PSO) To Analyze and Predict Crime Data", Journal of Advanced Research in Dynamic and Control Systems, Issue: 06,2018, Pages: 699-707

[14] Selvakumar, S & Inbarani, Hannah & Mohamed Shakeel, P. (2016). A hybrid personalized tag recommendations for social E-Learning system. 9. 1187-1199.

[15] P Hemkumarand, G Nagarajan"Current Fed Full Bridge Soft Switching Grid Connected Solar Based Push Pull Inverter"ARPN Journal of Engineering and Applied Sciences ,Vol-11 (13), pp8389-8394,2016.